

CORRECTION

Correction: FOXP4 differentially controls cold-induced beige adipocyte differentiation and thermogenesis

Fuhua Wang, Shuqin Xu, Tienan Chen, Shifeng Ling, Wei Zhang, Shaojiao Wang, Rujiang Zhou, Xuechun Xia, Zhengju Yao, Pengxiao Li, Xiaodong Zhao, Jiqui Wang and Xizhi Guo

There were errors in *Development* (2022) 149, dev200260 (doi:10.1242/dev.200260).

The location labels in Fig. 3D were incorrect. The corrected and original panels are shown below.

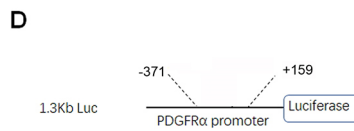


Fig. 3. (corrected). FOXP4 controls beige adipocyte differentiation by regulating *Pdgfra* transcription. (D) One putative FOXP4 binding site was detected –107 bp upstream of the *Pdgfra* gene transcription start site (TSS). Luciferase reporter assay validated the repressive activity of Foxp4 protein in *Pdgfra* gene transcription in HEK293T cells.

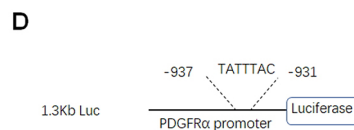


Fig. 3. (original). FOXP4 controls beige adipocyte differentiation by regulating *Pdgfra* transcription. (D) One putative FOXP4 binding site was detected –937 bp upstream of the *Pdgfra* gene transcription start site (TSS). Luciferase reporter assay validated the repressive activity of Foxp4 protein in *Pdgfra* gene transcription in HEK293T cells.

The legend for Fig. 7B quoted an incorrect target number. The corrected and original legends are shown below.

Fig. 7. (corrected). FOXP4 directly regulates the expression of *Cebpb* and *Pgc1a* during beige adipocyte thermogenic activation. (B) Heatmap of the 22 putative FOXP4-targeted gene expressions from the experiment shown in A. Chromatin occupancy analysis of ChIP-seq was conducted for SVF-derived beige adipocytes with an anti-Foxp4 antibody and 22 common targets were detected to overlap with RNA-seq results.

Fig. 7. (original). FOXP4 directly regulates the expression of *Cebpb* and *Pgc1a* during beige adipocyte thermogenic activation. (B) Heatmap of the 22 putative FOXP4-targeted gene expressions from the experiment shown in A. Chromatin occupancy analysis of ChIP-seq was conducted for SVF-derived beige adipocytes with an anti-Foxp4 antibody. Five common targets were detected to overlap with RNA-seq results.

In Fig. S6C, the heatmap was incorrect. The corrected and original figures are shown below.

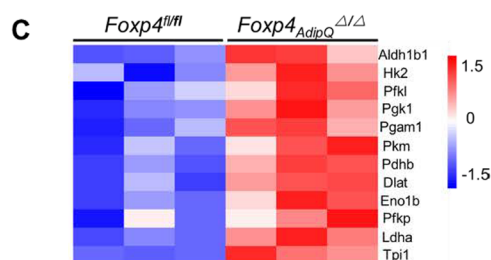


Fig. S6. (corrected). BAT thermogenesis in *Foxp4_{AdipQ}^{Δ/Δ}* mice upon cold exposure. (C) Heatmap depicting the mRNA levels of glycolytic genes in beige adipocytes from sWAT in *Foxp4_{AdipQ}^{Δ/Δ}* mice after one-week cold exposure at 4°C.

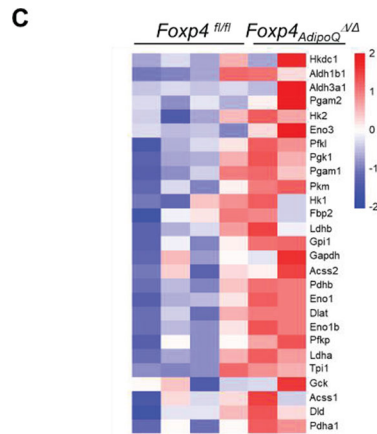


Fig. S6. (original). BAT thermogenesis in *Foxp4^{AdipoQ-Δ/Δ}* mice upon cold exposure. (C) Heatmap depicting the mRNA levels of glycolytic genes in beige adipocytes from sWAT in *Foxp4^{AdipoQ-Δ/Δ}* mice after one-week cold exposure at 4°C.

In Fig. S8, a panel was removed, so both the figure and legend have been updated. The corrected and original figures are shown below.

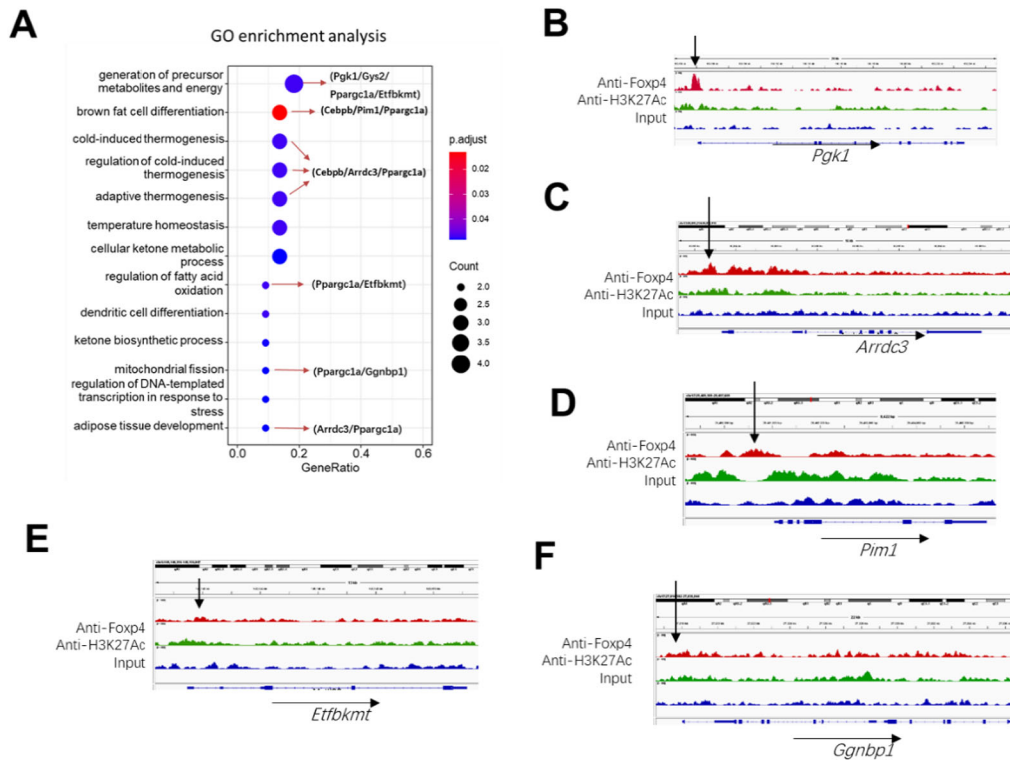


Fig. S8. (corrected). Crossover examinations of RNA-seq and ChIP-seq data to identify putative FOXP4 targeting genes. (A) GO enrichment analysis for several putative FOXP4-targeting genes. (B-F) ChIP-seq profile showed the FOXP4 binding sites (black arrows) within *Pgk1*, *Arrdc3*, *Pim1*, *Etfbkm1*, *Ggnbp1* gene regions.

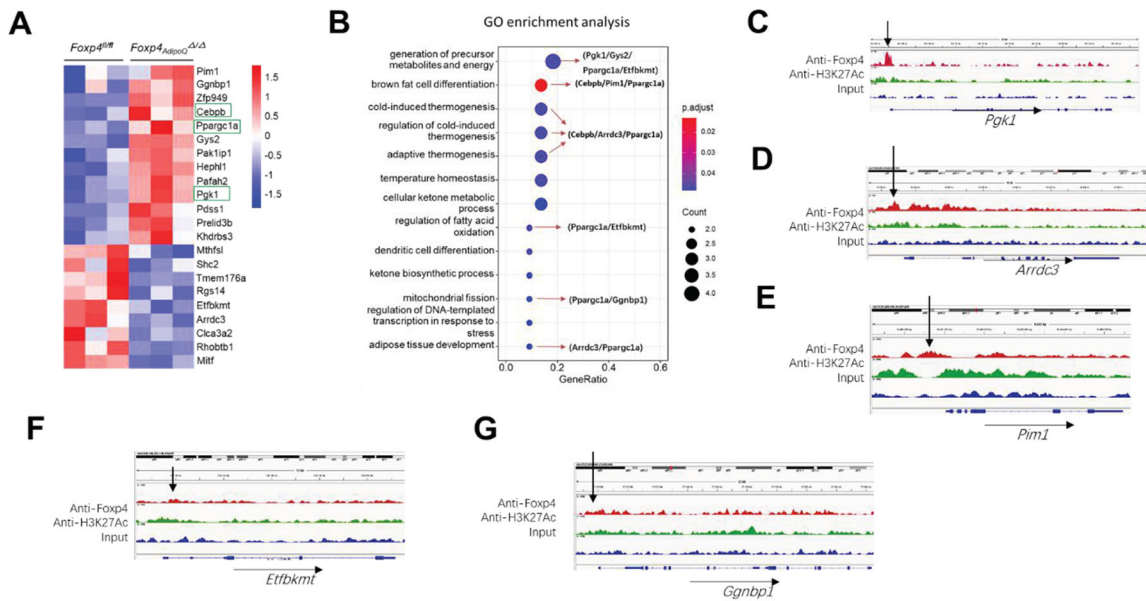


Fig. S8. (original). Crossover examinations of RNA-seq and ChIP-seq data to identify putative FOXP4 targeting genes. (A) Heatmap of thermogenic marker gene expressions by RNA-seq analysis in sWAT of *Foxp4^{AdipQ} Δ/Δ* mice under one-week 4°C challenge. (B) GO enrichment analysis for several putative FOXP4-targeting genes. (C-E) ChIP-seq profile showed the FOXP4 binding sites (black arrows) within *Pdgk1*, *Arrdc3*, *Pim1*, *Etfbkm1*, *Ggnbp1* gene regions.

Also, some values for *n* have been replaced in the updated Supplementary information.

Fig. S3B

Corrected

(B) Assessment of *Foxp4* mRNA expression in BAT and sWAT from mice by qPCR. *n*, 3~5.

Original

(B) Assessment of *Foxp4* mRNA expression in BAT and sWAT from mice by qPCR. *n*, 3.

Fig S3H

Corrected

(H) Oxygen consumption rate (OCR) was measured for brown adipocytes from (F). Uncoupled respiration was recorded after oligomycin inhibition of 1 ATP synthesis, and maximal respiration following stimulation with carbonyl cyanide 4-(trifluoromethoxy) phenylhydrazone (FCCP). *n*, 7.

Original

(H) Oxygen consumption rate (OCR) was measured for brown adipocytes from (F). Uncoupled respiration was recorded after oligomycin inhibition of ATP synthesis, and maximal respiration following stimulation with carbonyl cyanide 4-(trifluoromethoxy) phenylhydrazone (FCCP). *n*, 3.

Fig S3I

Corrected

(I) Quantitative analysis of basal and uncoupled OCR in (H). *n*, 7.

Original

(I) Quantitative analysis of basal and uncoupled OCR in (H). *n*, 3.

Fig S7B,D

Corrected

(B,D) qPCR analysis for thermogenic gene expressions in BAT (B) and sWAT (D) from CL-316,243-stimulated mice. *n*, 3.

Original

(B,D) qPCR analysis for thermogenic gene expressions in BAT (B) and sWAT (D) from CL-316,243-stimulated mice. *n*, 5.

Both the online full text and PDF versions of the paper have been corrected. We apologise to the readers for these errors and any inconvenience they may have caused.